

Field-asymmetric transverse magnetoresistance in a nonmagnetic quantum-size structure

A.A. Gorbatsevich^a, V.V. Kapaev^b, Yu.V. Kopaev^b,
I.V. Kucherenko^b, O.E. Omel'yanovskii^b, V.I. Tsebro^{b,1}

^a*Moscow Institute of Electronics, 103498 Moscow, Russia*

^b*P.N. Lebedev Physics Institute, Russian Academy of Sciences, 117924 Moscow,
Russia*

Abstract

A new phenomenon is observed experimentally in a heavily doped asymmetric quantum-size structure in a magnetic field parallel to the quantum-well layers – a transverse magnetoresistance which is asymmetric in the field (there can even be a change in sign) and is observed in the case that the structure has a built-in lateral electric field. A model of the effect is proposed. The observed asymmetry of the magnetoresistance is attributed to an additional current contribution that arises under nonequilibrium conditions and that is linear in the gradient of the electrochemical potential and proportional to the parameter characterizing the asymmetry of the spectrum with respect to the quasimomentum.

1. An artificially grown asymmetric quantum-size structure in a magnetic field oriented parallel to the quantum-well layers is a system with broken fundamental symmetries with respect to inversion of the coordinates and to time reversal. These symmetry breakings lead to unusual macroscopic properties. Specifically, it has been shown theoretically [1,2] that such a system can possess anomalously large photogalvanic and magnetoelectric effects. The large values of the photogalvanic effect were confirmed experimentally in Refs. 3 and 4.

In the present letter we report the observation of a fundamentally new phenomenon – a transverse magnetoresistance which is asymmetric with respect to the sign of the field – arising in an asymmetric quantum-size structure. The effect is observed in the case when a built-in lateral electric field exists in

¹ Author for correspondence (tsebro@sci.lebedev.ru).

the structure. This usually happens in a small region near the fused-in metal contact.

2. Our experimental GaAs/Al_xGa_{1-x}As ($x = 0.34$) nanostructure is a heavily doped single i-GaAs quantum well having average width (300Å) and bounded on both sides by $\sim 300\text{\AA}$ wide Al_xGa_{1-x}As barrier layers, uniformly doped with silicon to volume density $c_{Si} \sim 10^{18}\text{cm}^{-3}$. The well is separated from the doped barrier regions by i-Al_xGa_{1-x}As spacer layers $\sim 100\text{\AA}$ wide.

A quantum-mechanical calculation of the space-quantization energy levels in this geometry showed that there are three levels below the Fermi level E_F : E_1 , E_2 and E_3 , such that $E_F - E_1 \approx 32\text{ meV}$, $E_2 - E_1 = 5 \div 6\text{ meV}$, and $E_F - E_3 = 1 \div 5\text{ meV}$. The levels E_1 and E_2 are located slightly below the convex bottom of the quantum well, so that this structure can be viewed as a bilayer two-dimensional electronic system (see Fig. 1).

The electronic parameters of the system were determined from measurements of the Hall effect and Shubnikov-de Haas oscillations with the magnetic field oriented in a direction normal to the plane of the nanostructure. The experimental value of the Fermi energy is $E_F = (\hbar e/m^*c)(1/\Delta(1/H)) \approx 32\text{ meV}$ ($m^* = 0.067m_e$), and the two-dimensional charge-carrier density $n = (e/\pi\hbar c)(1/\Delta(1/H)) \approx 0,9 \cdot 10^{12}\text{cm}^{-2}$ was found to be approximately two times smaller than the carrier density determined from the Hall constant R_H in weak magnetic fields $n = 1/ecR_H \approx 1,9 \cdot 10^{12}\text{cm}^{-2}$. These data show that in accordance with the model calculation the carrier densities in the two bottom subbands are approximately equal, and the population of the third subband is extremely small because of the closeness of the bottom of this subband to the Fermi level.

The degree of asymmetry of the nanostructure can be judged according to the variation of the dispersion curves (Fig. 1c) and the shape of the Fermi contours (Fig. 1b) as a function of the magnetic field for each filled subband (charge-carrier motion is confined to the $x - y$ plane, and the magnetic field is directed along the y axis). One can see that despite the very small difference of the potential energy profile of the nanostructure to the left and right of the interfaces ($\sim 20\text{ meV}$), the magnetic field distorts the charge-carrier spectrum very strongly, deforming the Fermi contour along the x axis and leading to a very strong asymmetry of the dispersion curves $E(k_x)$.

3. The magnetoresistance measurements were performed by the standard four-contact method with dc current. The potential contacts were of two types: a) fused-in metallic (indium) contacts (in this case the sections of the near-contact region of the nanostructure with a built-in lateral electric field contribute to the measured electrical resistance), and b) lithographically prepared lateral contacts through etched-out extensions of the nanostructure itself (in

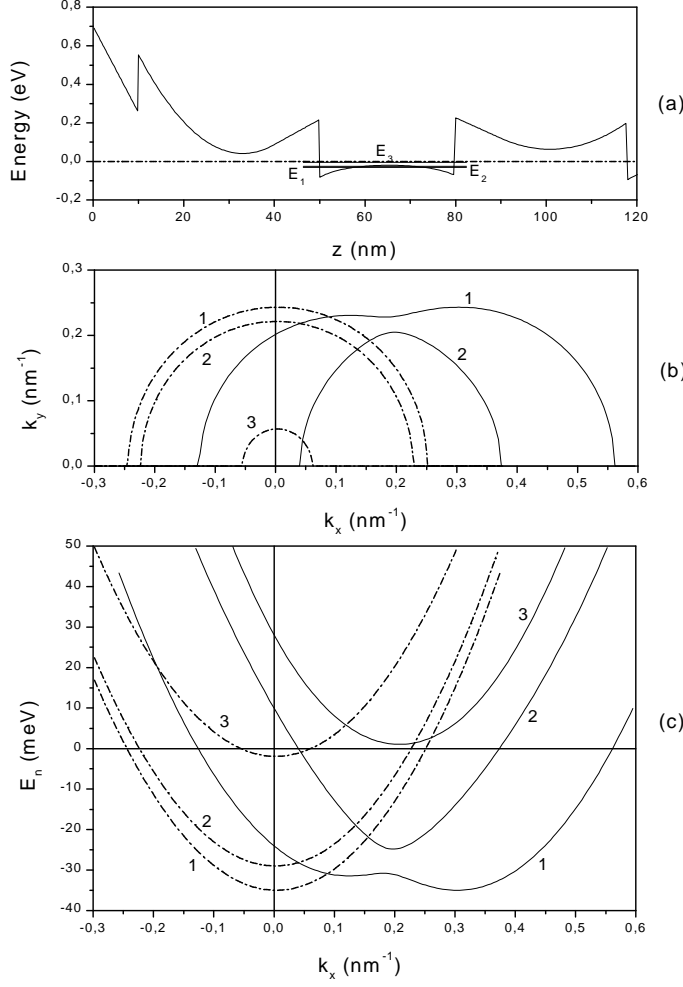


Fig. 1. Computed potential profile (a) of the conduction band bottom in the direction of the growth axis of the nanostructure; Fermi contours (b) and dispersion curves (c) for the three bottom subbands in 1 kOe (dot-and-dash curves) and 70 kOe (solid curves) magnetic fields.

this case the near-contact region with the built-in electric field does not make a contribution).

a) Fused-in indium potential contacts.

In this configuration the samples had a rectangular shape with the dimensions $\sim 2 \times 8$ mm and two current contacts fused in along the entire width of the sample and two $\sim 0,5$ mm fused-in potential contacts along one side of the sample, as shown in the upper part of Fig. 2.

Figure 2 shows the measurements of the transverse magnetoresistance at liquid-helium (curve a) and room (curve b) temperatures for both directions of the magnetic field. One can see that at liquid-helium temperature there is a strong negative transverse magnetoresistance $(\Delta R(H)/R(0)) \sim -0.4$ at $H =$

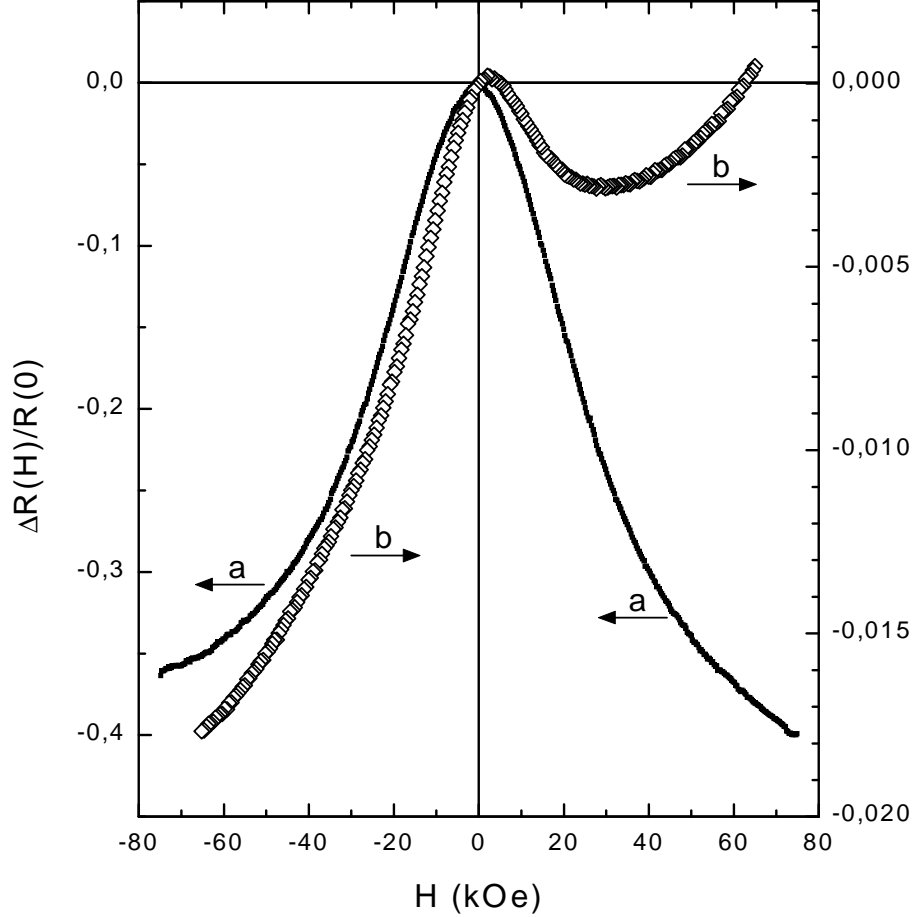


Fig. 2. Curves of the transverse magnetoresistance at liquid-helium (a) and room (b) temperatures for opposite orientations of the magnetic field. The geometry of the contacts is shown in the top portion of the figure.

75 kOe), which differs by $\sim 10\%$ for opposite orientations of the magnetic field, i.e., asymmetrically with respect to the direction of H . At room temperature the magnetoresistance decreases strongly in absolute magnitude to ~ 0.01 in strong magnetic fields, and it becomes asymmetric in H with respect to not only the magnitude but also the shape of the curves $\Delta R(H)/R(0)$ (curve b).

It should be emphasized particularly that neither the magnitude nor the sign of the asymmetry of the transverse magnetoresistance depends on the direction of the measuring current J through the sample for a fixed direction of the magnetic field, i.e., they are determined not by the relative orientation of the vectors \mathbf{H} and \mathbf{J} (provided that $\mathbf{H} \perp \mathbf{J}$) but by the relative orientation of the vector \mathbf{H} and the vector \mathbf{l} in the direction of the growth axis ($\mathbf{H} \perp \mathbf{l}$).

If the field dependence of the transverse magnetoresistance, measured for one direction of \mathbf{H} is subtracted from the corresponding dependence measured for the opposite direction, then in all cases there is a strictly linear dependence of the difference obtained on the absolute magnitude of H . This fact is il-

lustrated especially well by the data obtained at room temperature, where the magnetoresistance is small and the dependence $\Delta R(H)/R(0)$ has a pronounced nonmonotonic character (Fig. 3).

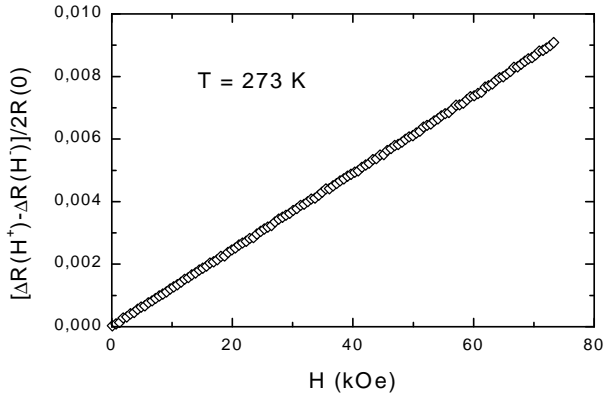


Fig. 3. Difference between the curves of the room-temperature transverse magnetoresistance measured for opposite directions of the magnetic field, plotted versus the absolute magnitude of the field.

We note that when the sample is rotated so that the vector \mathbf{H} is parallel to the current vector \mathbf{J} (the case of longitudinal magnetoresistance), the magnitude, and at high temperatures even the sign of the magnetoresistance change, but the important fact is that the asymmetry of the $\Delta R(H)/R(0)$ curves vanishes completely (Fig. 4).

b) Combined fused-in and lithographic potential contacts. The region of the nanostructure near the fused-in metallic contact is a region with the built-in lateral electric field². This electric field (\mathbf{E}_0), as will be noted below, confers to this region a nontrivial symmetry, as a result of which there arises a correction to the conductivity (or current) that is linear in the magnetic field. Since the observed asymmetry of the magnetoresistance is proportional to the magnitude and direction of \mathbf{E}_0 , it is obvious that the magnetoresistance asymmetry measured and described above is a difference effect, which is observable to the extent that the oppositely directed built-in electric fields \mathbf{E}_0^1 and \mathbf{E}_0^2 in the near-contact regions of the first and second potential contacts are unequal. For this reason, it was of interest to perform measurements of the transverse magnetoresistance on samples where only one fused-in potential contact is present on one side of the sample, since in this case an appreciable enhancement of the asymmetry effect should be expected.

² Simply depositing indium on the sample surface decrease the surface barrier (see Fig. 1) to ~ 0.5 V. This result in electron enrichment of the quantum well beneath the contact. On the other hand, when a metallic indium contact is fused in to some depth, the potential barrier approaches the quantum well, as a result of which the region beneath and in direct proximity to the contact becomes depleted of carriers. This depleted near-contact region possesses a very high resistivity, and for this reason, despite its small size (estimated as $\sim 1 \div 10 \mu m$), its field asymmetric contri-

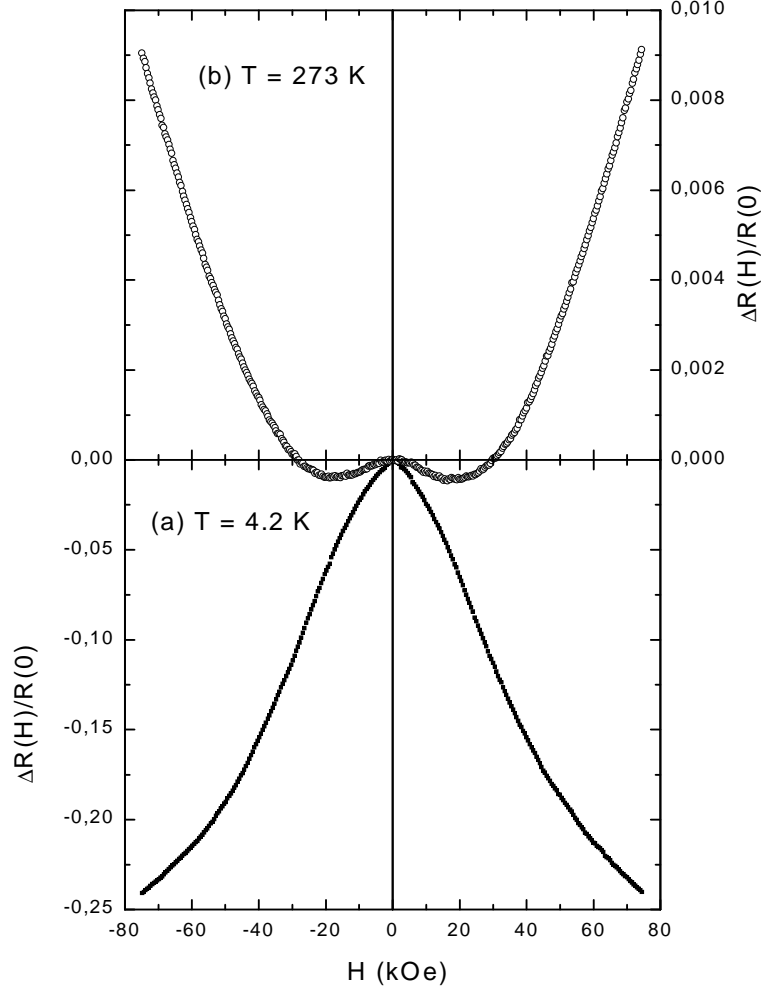


Fig. 4. Curves of the longitudinal magnetoresistance at liquid-helium (a) and room (b) temperatures for opposite orientations of the magnetic field.

The results of such measurements at liquid-helium and room temperatures are shown in Fig. 5. Three potential contacts were used (see top part of Fig. 5): one fused-in indium contact 1 and two lateral lithographic contacts 2 and 3, one of which was located close to the fused-in contact 1 so as to increase appreciably the contribution of the near-contact region of the fused-in contact 1 to the total measured magnetoresistance in measurements of the potential difference with contacts 1–2. The distance between contacts 1 and 2 was ~ 0.3 mm and the distance between contacts 2 and 3 was ~ 6 mm.

As one can see from the data presented in Fig. 5a in the case of the potential contacts 1–2 the asymmetry of the transverse magnetoresistance at $T = 4.2$ K increased appreciably and reached $\sim 50\%$ (curve 1a). In the case of the potential contacts 1–3 the asymmetry was $\sim 2\%$, in accordance with the ratio

tribution to the magnetoresistance turns out to be very considerable and determines the asymmetry of the transverse magnetoresistance of the sample as a whole.

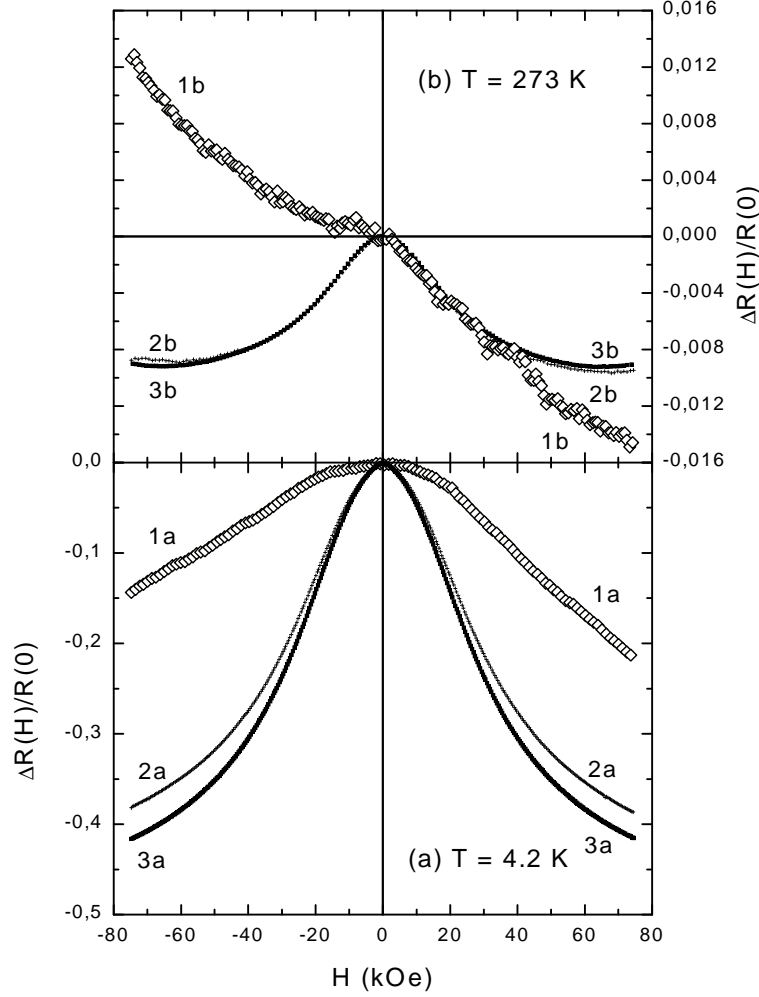


Fig. 5. Curves of the transverse magnetoresistance at liquid-helium (a) and room (b) temperatures in the case of combined potential contacts. Curves 1a and 1b were obtained with potential contacts 1–2; curves 2a, 2b and 3a, 3b were obtained with contacts 1–3 and 2–3, respectively.

of the distances between the contacts 1–2 and 1–3 (curve 2a). Finally, in the case of the potential contacts 2–3 the magnetoresistance curves are completely symmetric (curve 3a).

We note that the room temperature magnetoresistance (Fig. 5b) in the case of potential contacts 1–2 does not simply become even more asymmetric. It even becomes opposite in sign: positive for one direction of the magnetic field and negative for the other (see curve 1b).

4. The macroscopic symmetry of the asymmetric system of quantum wells in a magnetic field parallel to the layers is characterized by a t -odd polar vector [1,2]

$$\mathbf{T} \propto [\mathbf{HP}], \quad (1)$$

where \mathbf{H} is the external magnetic field, and \mathbf{P} is a polar vector characterizing the spatial asymmetry of the system and is directed perpendicular to the plane of the quantum wells. Physically, the vector \mathbf{T} is the toroidal moment density [5,6].

Since \mathbf{T} and the quasimomentum \mathbf{k} have the same transformation properties, the product of \mathbf{T} by \mathbf{k} is an invariant, and the energy spectrum, which can contain all possible invariants, is asymmetric in the quasimomentum:

$$E(\mathbf{k}) \neq E(-\mathbf{k}).$$

It is also known (see Refs. 1 and 2) on the basis of symmetry considerations that under nonequilibrium conditions there can exist a macroscopic current

$$\mathbf{j} = \beta \mathbf{T}, \quad (2)$$

where the coefficient β is due to the departure from equilibrium. If the source of disequilibrium is photoexcitation, the above-mentioned anomalously large photogalvanic effect is observed [3,4]. However, a relation between \mathbf{j} and \mathbf{T} similar to Eq. (2) can exist if the nonequilibrium is produced by an ordinary dissipative (Ohmic) current passed through the system. In this case, there exists in the system a gradient of the electrochemical potential, and the dissipative coefficient β is linear in the electric field \mathbf{E} :

$$\beta \propto \alpha(\mathbf{L}\mathbf{E}),$$

where α is a scalar and \mathbf{L} is a polar vector. In the samples investigated the vector \mathbf{L} is determined by the built-in electrostatic field in the near-contact space-charge region. The expression for the current (2) in this case can be rewritten in the form

$$\mathbf{j} = \alpha[\mathbf{P}\mathbf{H}](\mathbf{L}\mathbf{E}). \quad (3)$$

In a macroscopically nonuniform system \mathbf{E} is the gradient of the electrochemical potential. The current contribution (3) leads in an obvious manner to an anomalous contribution to the electrical conductivity, one which is asymmetric with respect to the magnetic field.

In the microscopic description of the effect, one must substitute into the general expression for the current density (where $E(\mathbf{k})$ is the energy spectrum and D is the \mathbf{k} -space dimension)

$$\mathbf{j} = \int \frac{\partial E(\mathbf{k})}{\partial \mathbf{k}} f(\mathbf{k}) \frac{d^D \mathbf{k}}{(2\pi)^D} \quad (4)$$

the distribution function $f(\mathbf{k})$ found from the kinetic equation

$$\left(\mathbf{v} \frac{\partial}{\partial \mathbf{r}} - \frac{e}{\hbar} \left(\mathbf{E} + \frac{1}{c} [\mathbf{v} \mathbf{H}] \right) \frac{\partial}{\partial \mathbf{k}} \right) f(\mathbf{k}, \mathbf{r}) = -\frac{f(\mathbf{k}, \mathbf{r}) - f^0(\mathbf{k}, \mathbf{r})}{\tau}, \quad (5)$$

where τ is the corresponding relaxation time, $f^0(\mathbf{k}, \mathbf{r})$ is the equilibrium distribution function, $\mathbf{E} = -\nabla\varphi(\mathbf{r})$ is the electric field, and $\mathbf{v} = \partial E(\mathbf{k})/\partial \mathbf{k}$ is the velocity of carriers with the spectrum $E(\mathbf{k})$ obtained by solving the Schrödinger equation.

For an asymmetric structure, similar to the one investigated in the present work, the quasiclassical energy spectrum to be substituted into Eq. (4) has the form

$$E(k_x, k_y) = E_n(k_x, k_y) + \varphi(x) = \frac{\hbar^2 k_y^2}{2m} + E_n(k_x) + \varphi(x), \quad (6)$$

where $E_n(k_x)$ is the size-quantized and magnetic-field-quantized energy spectrum, which in the general case can be easily obtained numerically (see Fig. 1c).

In a system with a built-in potential neither term on the left-hand side of Eq. (5) is small, generally speaking, and at equilibrium they exactly compensate one another. If the deviation from equilibrium is small, the current $j = n\mu\nabla F$ (where F is the electrochemical potential) flowing in the system can be taken as the corresponding small parameter. In this case the kinetic equation (5) can be solved by the perturbation method. It can be shown that the first-order correction to the distribution functions does not give a contribution to the electrical conductivity that is asymmetric with respect to the magnetic field. In the case of nondegenerate charge-carrier statistics, we have for the second-order correction introduced in the distribution function by the effect under study

$$f^{(2)} = -\frac{e^2 \tau^2}{\hbar T} f^{(0)} \left(\mathbf{E}_0 \frac{\partial}{\partial \mathbf{k}} \right) \left(\mathbf{v} \frac{\partial}{\partial \mathbf{r}} \right) F. \quad (7)$$

In this equation $\mathbf{E}_0 = -\nabla\varphi_0$ is the electric field vector of the built-in field in our system (near the metallic contact). Upon substitution of expression (7) into Eq. (4), the corresponding contribution to the current is different from zero only if the spectrum (6) is asymmetric with respect to the quasimomentum. The expression obtained in this manner for the current has the same form as expression (3), where the built-in field \mathbf{E}_0 enters as the vector \mathbf{L} .

References

- [1] A. A. Gorbatsevich, V. V. Kapaev, Yu. V. Kopaev, *JETP Lett.*, **57**, 580 (1993).
- [2] A. A. Gorbatsevich, V. V. Kapaev, Yu. V. Kopaev, *Ferroelectrics*, **161**, 303 (1994).
- [3] Yu. A. Aleshchenko, I. D. Voronova, S. P. Grishechkina *et al.*, *JETP Lett.*, **58**, 384 (1993).
- [4] O. E. Omel'yanovskii, V. I. Tsebro, V. I. Kadushkin, *JETP Lett.*, **63**, 209 (1996).
- [5] V. L. Ginzburg, A. A. Gorbatsevich, Yu. V. Kopaev, B. A. Volkov, *Sol. St. Comm.*, **50**, 339 (1984).
- [6] A. A. Gorbatsevich, *Zh. Eksp. Teor. Fiz.*, **95**, 1467 (1989) [*Sov. Phys. JETP*, **68**, 847 (1989)].

Translated by M. E. Alferieff